Isothermal Mechanical Response of Shape Memory Polymer (SMP)-Based Hybrid Models and SMP-Composites

A. Bhattacharyya[1]

Smart Materials and MEMS Laboratory[2]
Department of Applied Science
University of Arkansas at Little Rock 2801 South University,
ETAS 575 Little Rock, AR 72204-1099, USA

ABSTRACT

This paper has addressed the issue of isothermal uniaxial mechanical response of a shape memory polymer (SMP) in series and parallel arrangements with a spring, dashpot, a Maxwell solid and a Kelvin solid. It is shown analytically that four models – the SMP- spring series hybrid, SMP-spring parallel hybrid, SMP-Kelvin solid series hybrid and the SMP-Maxwell solid parallel hybrid – demonstrate an effective response analytically identical to that of a shape memory polymer. Explicit expressions for the creep strain and damping capacity are provided for the SMP-spring hybrids. Parametric studies for the SMP-spring series hybrid and the SMP-spring parallel hybrid are then used to suggest design strategies for SMP-based composite laminates and aligned fiber composites.

Key Words: Shape memory polymers, SMP, composites, viscoelasticity, shape memory strain, damping

1. INTRODUCTION

Smart materials research encompasses a wide variety of materials; some of these are shape memory alloys, piezoelectric materials, ferroelectric materials, magnetostrictive materials, polymeric gels. A recent addition to that list is shape memory polymers (SMP). The SMPs are a class of polyurethanes that are capable of undergoing significant deformations when subjected to a thermomechanical input. The deformations are recoverable, although with some hysteresis. This class of deformations is commonly referred to in the literature as the shape memory effect (SME), and in that sense, the response of the SMP is

[1] Tel: 501 569 8027 , Fax: 501 569 8020 , Email: axbhattachar@ualr.edu
[2] http://mems.appsci.ualr.edu

very similar to those of shape memory alloys (SMAs). Representative contributions in SMP research are those due to Tobushi *et al.* (1997), Liang, Rogers and Malafeew (1991), Tobushi, Hayashi and Lin (1994), Gordon (1994), Tobushi *et al.* (1996) and Bhattacharyya and Tobushi (2000).

A linear viscoelastic model including a friction element was proposed for the SMP by Tobushi *et al.* (1997), see Figure 1. While the SME is no doubt a notable feature of SMPs, these materials also possess significant damping properties. In fact, Bhattacharyya and Tobushi (2000), in their analysis of the isothermal mechanical response of the SMP viscoelastic model proposed by Tobushi *et al.* (1997), proved analytically that above a certain threshold frequency, the damping seemed to be independent of the shape memory effect. Further, they also demonstrated that above this threshold frequency, the SMP damping capacity vs. temperature relation is non-monotonic, with the damping capacity reaching a maximum at the glass transition temperature.

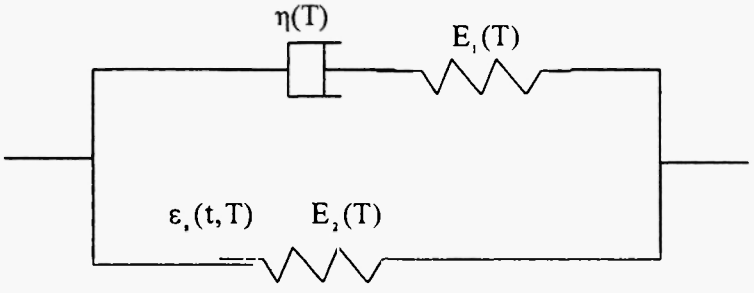

Fig. 1: The schematic of the shape memory polymer (SMP) rheological model.

The current work is motivated by several issues. For example, if the SMP is used along with an inactive constituent in a two-phase composite, to what extent would the properties of the SMP translate to that of the composite? A specific example is a glass fiber-reinforced SMP composite that will potentially demonstrate a significant SME and an excellent damping property (due to the SMP) as well as benefit from the reinforcing effects of an inactive but a stiff second phase (due to the glass fibers). An ideal approach to design such composites is to combine modeling with corresponding experiments. This of course implies that the multiaxial constitutive response of the SMP needs to be developed for input into any analysis of the SMP-based composite response. On the other hand, one-dimensional (1D) constitutive models may be used to gain some insight into the response of SMP-based composites before multiaxial constitutive models for the SMP are developed.

In a situation as described above, it is often of interest to consider the classical approach of "constructing" hybrid rheological models that are 1D in stress and strain. The new ingredient, which has not been considered before, is the SMP rheological element as a model component. Thus, for example, an SMP-spring series hybrid may be used to study the response of a SMP-elastic composite laminate subjected to uniaxial loading

perpendicular to the plane of the laminate (see Figure 2a). On the other hand, a spring-SMP parallel hybrid may be used to study the uniaxial loading (along the fiber direction) of an aligned elastic fiber-reinforced SMP composite (see Figure 2b). Hybrid models are also useful from a practical standpoint. The response of the SMP-based composites as obtained from experiments may seek to be simulated by different SMP-based hybrid models, and whichever model matches the experimental results "best" may be used in engineering design to represent the particular composite response it simulates. In this paper, we focus on several hybrid models, which follow by combining an SMP element with, in turn, (i) an elastic element, (ii) a dashpot, (iii) a Maxwell solid, and (iv) a Kelvin solid (see Figure 3). For each hybrid model, both series and parallel combinations are considered. General expressions for the loss angle and the creep response to a constant stress input are given for all the hybrid models, and analytical observations made on their effective response. As well, explicit expressions are given for some selected models and, finally, parametric studies are carried out for the SMP-spring hybrid models. It is worthwhile to note that these results are based on the specific linear viscoelastic model proposed by Tobushi *et al.* (1997). These results can only be applied to SMPs with low strain. While that is indeed a limitation, the analytical results are quite useful in studying the trends in the mechanical response of the SMP-based hybrid models and composites. However, for large strain applications, the linear model may be replaced by the nonlinear constitutive model proposed recently by Tobushu, Okumura, Hayashi and Ito (2001). We propose to study the impact of the non-linearity and large strain on SMP-based hybrid models in the future.

This paper is organized in seven sections. The rheological model of the SMP is recapitulated in Section 2. The governing equations for the SMP-based hybrid models are given in Section 3. The solution for the isothermal constant stress creep response (that demonstrates the shape memory strain acquired at a given temperature) as well as the damping are addressed in Section 4. In Section 5, explicit expressions for the

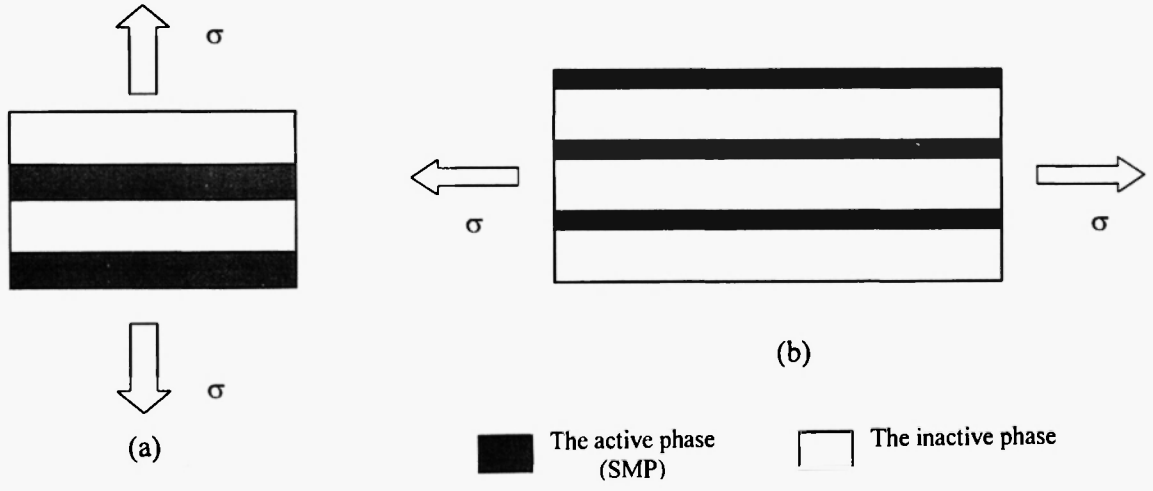

Fig. 2: Schematic of a two-phase composite with an active (SMP) and an inactive phase, in a (a) laminate arrangement, (b) parallel fiber-matrix arrangement.

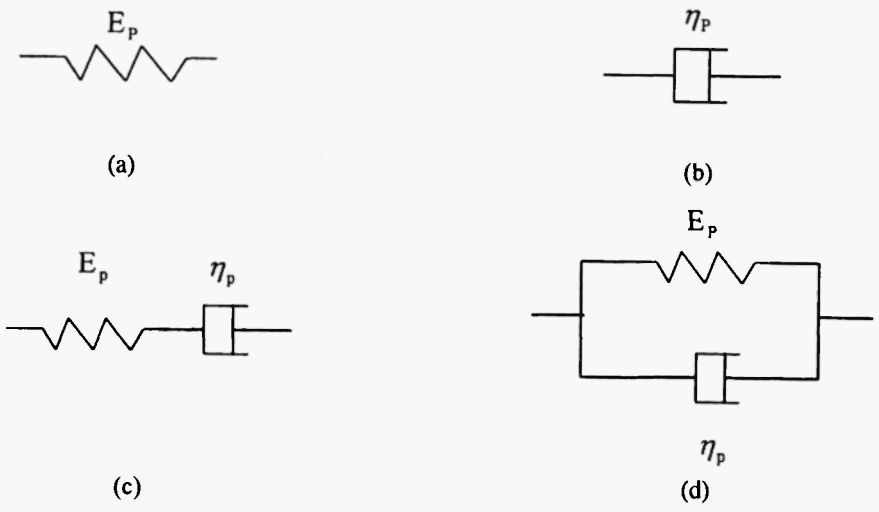

Fig. 3: A schematic of (a) a spring, (b) a dashpot, (c) a Maxwell solid, and (d) a Kelvin solid, with their associated parameters.

creep strain and loss angle for the spring-SMP hybrid models are given. Results and parametric studies are given in Section 6 whereas conclusions are given in Section 7. In the entire study, inertia effects will not be considered and the theory will be developed within the context of small deformations and deformation gradients.

2. THE RHEOLOGICAL MODEL OF A SHAPE MEMORY POLYMER

A rheological model for a shape memory polymer (SMP) was proposed by Tobushi *et al.* (1997) and is shown in Figure 1. The model was developed based on tensile tests of SMP thin films, and consists of two springs, a dashpot and a friction element. In absence of the friction element, the resulting 3-element model is a linear viscoelastic solid that has been categorized as a member of Group I models, all exhibiting a solid-like character with retarded elasticity (Findley, Lai and Onaran, 1976). The friction element is used to capture the shape memory effect of the polymer. This model has certain interesting features, uncovered in the analysis of Bhattacharyya and Tobushi(2000).

Consider the SMP to be subjected to a stress, $\sigma^{SMP}(t)$ (where "t" is time). The SMP will have a creep strain, $\varepsilon^{SMP}(t)$, defined as

$$\varepsilon_c^{SMP}(t) = \varepsilon^{SMP}(t) - \frac{\sigma^{SMP}(t)}{E(T)} , \tag{1}$$

where $\varepsilon^{SMP}(t)$ is the total SMP strain and E(T) is the Young's modulus of the SMP (defined later). A component of this creep strain is irrecoverable and is denoted as $\varepsilon_s(t,T)$ (strain in the friction element). The value of this strain during $t > \bar{t}$ was proposed to have the following form (Tobushi *et al.*, 1997)

$$\varepsilon_s(t,T)=\left\{\begin{array}{lll} 0 & \text{when} & \varepsilon_c^{SMP}(t)<\varepsilon_L(T) \\ C(T)\left(\varepsilon_c^{SMP}(t)-\varepsilon_L(T)\right) & \text{when} & \varepsilon_c^{SMP}(t)>\varepsilon_L(T)\ ,\ \dot{\varepsilon}_c^{SMP}(\bar{t})>0 \\ \varepsilon_s(\bar{t},t) & & \dot{\varepsilon}_c^{SMP}(\bar{t})>0 \end{array}\right\} \text{ during } t>\bar{t}\ , \quad (2)$$

where C(T) and $\varepsilon_L(t)$ are positive temperature-dependent parameters, $0 \le C(T) < 1$, $\varepsilon_L(T) > 0$ (Tobushi *et al.*, 1997), and the superimposed time derivative, i.e. $\dot{\varepsilon}_c^{SMP} \equiv d\varepsilon_c^{SMP}/dt$. The irrecoverable creep strain, $\varepsilon_s(t,T)$, is responsible for the shape memory effect in the SMP. Since the differential equation relating the total SMP stress, $\sigma^{SMP}(t)$, to the total SMP strain, $\varepsilon^{SMP}(t)$, as suggested by Tobushi *et al.* (1997) involves $\varepsilon_s(t,T)$ (see Equation 2), there are three possible expressions for the differential equation. All three expressions may be summarised as

$$\dot{\varepsilon}^{SMP}(t)=\frac{\dot{\sigma}^{SMP}(t)}{E(T)}+\frac{\sigma^{SMP}(t)}{\mu_{eff}(T,C)}-\frac{\varepsilon^{SMP}(t)}{\lambda_{eff}(T,C)}+\frac{\varepsilon_{s,eff}(T,C)}{\lambda_{eff}(T,C)}\ , \qquad t>\bar{t}\ , \quad (3)$$

where the parameters, $\mu_{eff}(T,C)$, $\lambda_{eff}(T,C)$ and $\varepsilon_{s\,eff}(T,C)$, are defined as

$$\mu_{eff}(T,C)=\mu(T)\left[1-\frac{E_2(T)C}{E(T)}\right]^{-1}\ , \qquad \lambda_{eff}(T,C)=\lambda(T)\left[1-C\right]^{-1}\ , \quad t>\bar{t}\ , \quad (4)$$

$$\varepsilon_{s,eff}(T,C)=\left\{\begin{array}{ll} \varepsilon_s(\bar{t},T) & \text{when} \quad \dot{\varepsilon}_c^{SMP}(\bar{t})<0 \\ -\dfrac{C\,\varepsilon_L(T)}{1-C} & \text{otherwise} \end{array}\right. , \quad (5)$$

and

$$C=\left\{\begin{array}{ll} 0 & \text{when} \quad \varepsilon_c^{SMP}(\bar{t})<\varepsilon_L(T) \text{ or when } \dot{\varepsilon}_c^{SMP}(\bar{t})<0 \\ \hat{C}(T) & \text{when} \quad \varepsilon_c^{SMP}(\bar{t})>\varepsilon_L(T)\ ,\ \dot{\varepsilon}_c^{SMP}(\bar{t})>0 \end{array}\right. \quad (6)$$

Finally, the parameters, E(T), $\mu(T)$ and $\lambda(T)$ (used in Equations 1-5), are the elastic modulus, coefficient of viscosity and the retardation time respectively of the SMP, defined as

$$E(T)=E_1(T)+E_2(T)\ , \qquad \mu(T)=\frac{\eta(T)E(T)}{E_1(T)}\ , \qquad \lambda(T)=\frac{\mu(T)}{E_1(T)}\ , \quad (7)$$

where the parameters, $E_1(T), E_2(T)$ and $\mu(T)$ are positive temperature-dependent values of the SMP rheological model parameters.

3. THE GOVERNING EQUATIONS FOR THE SMP-BASED HYBRID MODELS

The governing equations for the SMP-based hybrid models will be derived based on the composite laminate and the aligned fiber composite arrangements as shown in Figure 2. We denoted the active phase (SMP) with the subscript "A" and the inactive phase (any of Figure 3) with the subscript "IA". The composite laminate suggests a SMP-inactive phase series hybrid model where the stress and strain in the constituents are related as

$$\sigma = \sigma_A = \sigma_{IA} \quad , \quad \varepsilon = V_A\, \varepsilon_A + V_{IA}\, \varepsilon_{IA} \quad . \tag{8}$$

The aligned fiber composite suggests a SMP-inactive phase parallel hybrid model with stress and strain components related as

$$\sigma = V_A\, \sigma_A + V_{IA}\, \sigma_{IA} \quad , \quad \varepsilon = \varepsilon_A = \varepsilon_{IA} \quad . \tag{9}$$

Equations 9 and 8 are subject to the restriction that

$$V_A + V_{IA} = 1 \quad . \tag{10}$$

The total stress-total strain relation for each hybrid model may now be derived using Equation 3, either of Equation 8 or 9 and the appropriate constitutive response of the inactive phase (see Fig. 3 and refer to Findley, Lai and Onaran, 1976). The governing equations for all SMP-based hybrid models can be cast into the following differential form

$$P(T,C,D)\,\sigma(t) = Q(T,C,D)\left[\varepsilon(t) - \varepsilon_s^{total}(T,C)\right] \quad , \tag{11}$$

where $D \equiv \dfrac{d}{dt}$ is the time operator, while $P(T,C,D)$ and $Q(T,C,D)$ are differential operators relating the stress, $\sigma(t)$, to the expression, $\varepsilon(t) - \varepsilon_s^{total}(T,C)$. Specifically,

$$\begin{aligned} P(T,C,D) &= \alpha_1(T,C)D^2 + \alpha_2(T,C)D + \alpha_3(T,C) \ , \\ Q(T,C,D) &= \beta_1(T,C)D^2 + \beta_2(T,C)D + \beta_3(T,C) \ , \end{aligned} \tag{12}$$

where the parameters, α_i (T,C), β_i (T,C) (i = 1 , 2 , 3) and ε_s^{total}(T,C) (collectively referred to hereafter as the "model parameters") have expressions specific to the model that is being considered.

3.1 The Shape Memory Polymer

The specific expressions of the model parameters for the shape memory polymer (SMP) follow by rearranging Equation 3 in the form of Equation 11 where

$$\alpha_1(T,C)=0 \quad , \quad \alpha_2(T,C)=\frac{1}{E(T)} \quad , \quad \alpha_3(T,C)=\frac{1}{\mu_{eff}(T,C)} \quad ,$$
$$\beta_1(T,C)=0 \quad , \quad \beta_2(T,C)=1 \quad , \quad \beta_3(T,C)=\frac{1}{\lambda_{eff}(T,C)} \quad , \tag{13}$$
$$\varepsilon_s^{total}(T,C)=\varepsilon_{s,eff}(T,C) \quad .$$

3.2 SMP-based hybrid models

In this section, we shall consider a linear spring, a dashpot, a Maxwell solid and a Kelvin solid (all shown in Figure 3 with their components), in turn, connected with a SMP element in series (appropriately weighted with volume fractions; see Equation 8) and in parallel (see Equation 9). For each of these SMP-based hybrid models, the overall model parameters and the creep strain of the SMP have been derived. We have also derived the expression for the creep strain of the SMP as it is needed to determine ε_s (t,T) (see Equation 2). The expressions for the spring-SMP models are given below whereas the expressions for the dashpot-SMP, Maxwell-SMP and Kelvin-SMP models are given in Appendix A1.

3.2.1 The spring-SMP series hybrid

$$\alpha_1(T,C)=0 \quad , \quad \alpha_2(T,C)=\frac{V_A}{E(T)}+\frac{V_{IA}}{E_p} \quad , \quad \alpha_3(T,C)=\frac{1}{\mu_{eff}(T,C)}\left[V_A+V_{IA}\frac{E_{2,eff}(T,C)}{E_p}\right] \quad ,$$
$$\beta_1(T,C)=0 \quad , \quad \beta_2(T,C)=1 \quad , \quad \beta_3(T,C)=\frac{1}{\lambda_{eff}(T,C)} \quad , \tag{14}$$
$$\varepsilon_S^{total}(T,C)=V_A\varepsilon_{s\,eff}(T,C) \quad ,$$

$$\varepsilon_c^{SMP}(t)=\begin{cases}0 & \text{when} \quad V_A=0\\ \dfrac{1}{V_A}\left[\varepsilon(t)-\dfrac{V_{IA}}{E_p}\sigma(t)\right]-\dfrac{\sigma(t)}{E(T)} & \text{when} \quad V_A\neq 0\end{cases} \quad . \tag{15}$$

3.2.2 The spring-SMP parallel hybrid

$$\alpha_1(T,C)=0 \quad , \quad \alpha_2(T,C)=\frac{1}{V_A E(T)+V_{IA}E_p} \quad , \quad \alpha_3(T,C)=\frac{1}{\mu_{eff}(T,C)}\left[V_A+V_{IA}\frac{E_p}{E(T)}\right]^{-1} \quad ,$$

$$\beta_1(T,C)=0 \quad , \quad \beta_2(T,C)=1 \quad , \quad \beta_3(T,C)=\frac{1}{\lambda_{eff}(T,C)}\cdot\frac{V_A+V_{IA}\dfrac{E_p}{E_{2\,eff}(T,C)}}{V_A+V_{IA}\dfrac{E_p}{E(T)}} \quad , \tag{16}$$

$$\varepsilon_s^{total}(T,C)=\frac{V_A}{V_A+V_{IA}\dfrac{E_p}{E_{2,eff}(T,C)}}\varepsilon_{s,eff}(T,C) \quad ,$$

$$\varepsilon_c^{SMP}(t)=\begin{cases}0 & \text{when} \quad V_A=0\\ \left[1+\dfrac{V_{IA}}{V_A}\dfrac{E_p}{E(T)}\right]\varepsilon(t)-\dfrac{\sigma(t)}{V_A E(T)} & \text{when} \quad V_A\neq 0\end{cases} . \tag{17}$$

Note that among the eight models considered in this section, four of those can follow directly by replacing the SMP model parameters (Equation 13) by the corresponding hybrid model parameters. These four models are: (i) spring-SMP series hybrid, (ii) Kelvin solid- SMP series hybrid, (iii) spring-SMP parallel hybrid, and (iv) Maxwell solid-SMP parallel hybrid. Therefore, these four hybrid models have an effective response analytically identical to that of a shape memory polymer. Before closing this section, we point out that in addition to simulating the uniaxial response of two-phase composites, the hybrid models can also be used to simulate experimental results for two-phase composites with a SMP and an inactive phase with *arbitrary phase distribution.* In that case, the model parameters will simply represent the" composite" parameters, once we drop the restriction imposed by Equation 10 and set V_A = 1 and V_{IA} = 1 in Equations 8 and 9 respectively.

4. ISOTHERMAL, CONSTANT STRESS CREEP RESPONSE AND PERIODIC LOADING

In general, it is of interest to know to what extent the properties of the SMP carry over to the overall response of the hybrid models. In particular, the two principal fundamental SMP properties – shape memory strain and damping – are of interest. The analytical solutions for the isothermal constant stress creep response and isothermal periodic loading for the SMP-based hybrid models will yield information on the overall shape memory strain and overall damping respectively. These solutions are given next. In either case, we shall consider the following initial conditions for the overall stress and strain

$$\varepsilon(t)=0 \quad . \quad \sigma(t)=0 \qquad \text{at} \qquad t=0 \; . \tag{18}$$

Also, in order to exclude residual stress states, we shall assume that the stress and strain of the constituent elements of the SMP-based hybrid models (including the friction element) are zero at $t = 0$. Note that due to the assumption of an isothermal response, Equation 11 is a linear differential equation having an analytical solution.

4.1 Isothermal, constant stress creep response

A constant tensile stress input, σ_0, is applied over the duration, $0 < t \leq t_b$; thus

$$\sigma(t) = \begin{cases} \sigma_0 & 0 < t \leq t_b \\ 0 & t > t_b \end{cases}, \qquad \sigma_0 > 0$$

The total creep strain, $\varepsilon_c(t)$, is defined as

$$\varepsilon_c(t) = \varepsilon(t) - \varepsilon_{el}(t) \ , \tag{20}$$

where $\varepsilon(t)$ and $\varepsilon_{el}(t)$ the total strain and the total elastic strain respectively. The total strain, $\varepsilon(t)$, will follow from the solution of Equation 11. Therefore, the solution for the SMP response and that of four hybrid models (Sections 3.2.1, 3.2.2, A1.3, and A1.5) is given by

$$\varepsilon(t) = \varepsilon_s^{total}(T,C) + \left[\varepsilon(\bar{t}^{\,+}) - \varepsilon_s^{total}(T,C)\right] e^{-\beta_3(T,C)(t-\bar{t})} + \frac{\alpha_3(T,C)}{\beta_3(T,C)}\sigma(t)\left[1 - e^{-\beta_3(T,C)(t-\bar{t})}\right] \quad , \quad t > \bar{t} \ , \tag{21}$$

whereas for two other models (Sections A1.1 and A1.2), we have

$$\varepsilon(t) = \varepsilon(\bar{t}^{\,+}) + \frac{\alpha_3(T,C)}{\beta_2(T,C)}\sigma(t)(t-\bar{t}) + \frac{1}{\beta_2(T,C)}\left\{\dot{\varepsilon}(\bar{t}^{\,+}) - \frac{\alpha_3(T,C)}{\beta_2(T,C)}\sigma(t)\right\}\left[1 - e^{-\beta_2(T,C)(t-\bar{t})}\right] \ , \quad t > \bar{t} \ , \tag{22}$$

and for the remaining two models (Sections A1.4 and A1.6), we have

$$\varepsilon(t) = \varepsilon_s^{total}(T,C) + \frac{\alpha_3(T,C)}{\beta_3(T,C)}\sigma(t) + \frac{\dot{\varepsilon}(\bar{t}^{\,+}) - \psi_2(T,C)\left(\varepsilon(\bar{t}^{\,+}) - \varepsilon_s^{total}(T,C) - \frac{\alpha_3(T,C)}{\beta_3(T,C)}\sigma(t)\right)}{\psi_1(T,C) - \psi_2(T,C)} e^{\psi_1(T,C)(t-\bar{t})} \tag{23}$$

$$- \frac{\dot{\varepsilon}(\bar{t}^{\,+}) - \psi_1(T,C)\left(\varepsilon(\bar{t}^{\,+}) - \varepsilon_s^{total}(T,C) - \frac{\alpha_3(T,C)}{\beta_3(T,C)}\sigma(t)\right)}{\psi_1(T,C) - \psi_2(T,C)} e^{\psi_2(T,C)(t-\bar{t})} \quad , \quad t > \bar{t}$$

$$\psi_1(T,C) = \frac{-\beta_2(T,C) + \sqrt{\beta_2^2(T,C) - 4\beta_1(T,C)\beta_2(T,C)}}{2\beta_1(T,C)}$$
$$\psi_2(T,C) = \frac{-\beta_2(T,C) - \sqrt{\beta_2^2(T,C) - 4\beta_1(T,C)\beta_2(T,C)}}{2\beta_1(T,C)} \quad . \tag{24}$$

Note that the initial conditions, $\varepsilon(\bar{t}^+)$ and $\dot{\varepsilon}(\bar{t}^+)$, used in Equations 21, 22 or 23 are at $t = \bar{t}^+$, where we define $\varepsilon(\bar{t}^+) = \lim_{\Delta \to 0} \varepsilon(\bar{t} + \Delta)$ and $\dot{\varepsilon}(\bar{t}^+) = \lim_{\Delta \to 0} \dot{\varepsilon}(\bar{t} + \Delta)$, Δ being a very small positive quantity (i.e. $0 < \Delta << 1$). In that context, an alternative definition is

$$\varepsilon(\bar{t}^+) = \varepsilon(\bar{t}) + \Delta\varepsilon(\bar{t}) \quad , \qquad \dot{\varepsilon}(\bar{t}^+) = \dot{\varepsilon}(\bar{t}) + \Delta\dot{\varepsilon}(\bar{t}) \tag{25}$$

where $\Delta\varepsilon(\bar{t})$ and $\Delta\dot{\varepsilon}(\bar{t})$ are the jump in the total strain and the total strain rate respectively during the time interval, $\bar{t} \le t \le \bar{t}^+$ (possible due to a change in the piecewise constant stress input and/or the friction element becoming active/inactive). The procedure to determine $\Delta\varepsilon(\bar{t})$ and $\Delta\dot{\varepsilon}(\bar{t})$ has been demonstrated for the dashpot-SMP series model in the Appendix A2. An identical approach may be used for the similar models, For later use (Section 5), we provide the following specific results

$$\Delta\varepsilon(\bar{t}) = \frac{\alpha_2(T,C)}{\beta_2(T,C)}\Delta\sigma(\bar{t}) \quad , \qquad \Delta\dot{\varepsilon}(\bar{t}) = 0 \quad , \tag{26}$$

for the SMP, spring-SMP series and parallel hybrid models.

The elastic strain, $\varepsilon_{el}(t)$ (see Equation 20), for the stress input given in Equation 19 may be written as

$$\varepsilon_{el}(t) = \varepsilon_{el}(\bar{t}^+) = \varepsilon_{el}(\bar{t}) + \Delta\varepsilon_{el}(\bar{t}) = \varepsilon_{el}(\bar{t}) + \Delta\varepsilon(\bar{t}) \qquad , \qquad t > \bar{t}. \tag{27}$$

For the specific stress input given in Equation 19, the total strain, $\varepsilon(t)$, over the entire time range can be developed from either Equations 21, 22 or 23 (depending on the model under consideration), and the creep strain will follow from Equation 20. The details of the approach have been summarized in the flowchart given in Figure 5. The resulting specific expressions for the spring-SMP models will be given in Section 5.

4.2 Isothermal, periodic loading

We now consider a periodic strain with an amplitude, ε_0^B, and a frequency, ω, to be superimposed over a constant strain, ε_0^A, such that the total strain will have the form, $\varepsilon_0^A + \varepsilon_0^B \cos(\omega t)$. An alternative approach is to write the strain as

$$\varepsilon(t) = \varepsilon_0^A + \varepsilon_0^A e^{i\omega t} \quad , \qquad \varepsilon_0^A > \varepsilon_0^B > 0, \tag{28}$$

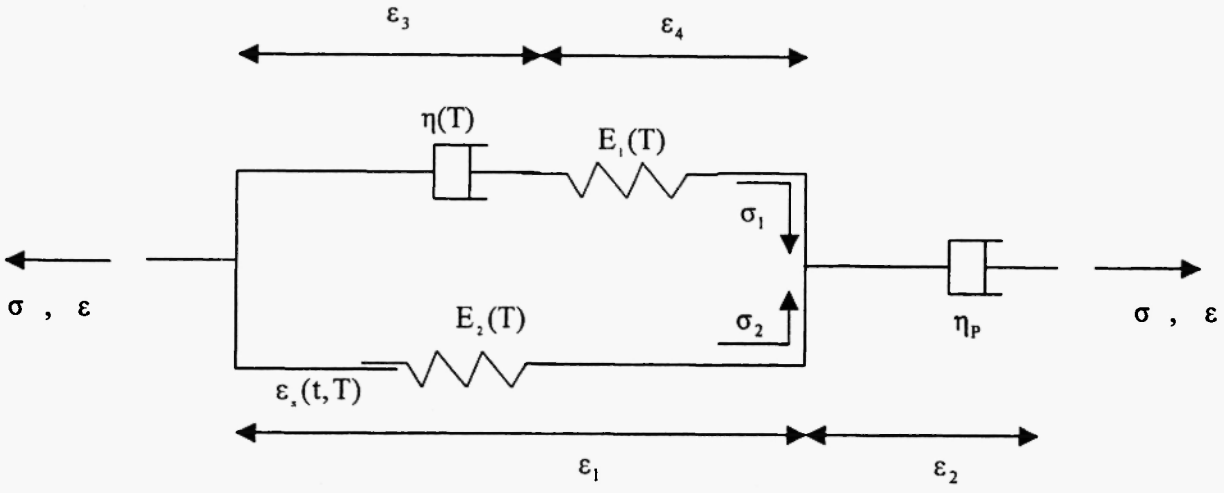

Fig. 4: A schematic of the SMP-dashpot series hybrid model showing the variables used for the stresses and strains in the constituent elements. 5. The flowchart for the computational procedure.

where $i = \sqrt{-1}$; note we have imposed the requirement, $\varepsilon_0^A > \varepsilon_0^B > 0$, to guarantee a globally extensional stress state at all times. It shall be understood that the strain is given by the real part of the expression on the right of Equation 28. Such a representation allows the use of complex variable techniques to solve for the periodic part of the stress response (see Findley, Lai and Onaran, 1976). The response of a viscoelastic solid to a periodic strain input as in Equation 28 will have a stress response with a short-term transient component, $\sigma_0^A(t)$, and a long term periodic component, $\sigma_0^B e^{i(\omega t+\delta)}$. The total stress then is

$$\sigma(t) = \sigma_0^A(t) + \sigma_0^B e^{i(\omega t+\delta)} \quad , \tag{29}$$

where δ is the phase angle (or the loss angle); if δ is positive (negative), then the periodic component of the stress leads (lags) the periodic component of the imposed periodic strain. Equations 28 and 29 give us the relaxation storage modulus, $E_{storage}$, and the relaxation loss modulus, E_{loss}. These follow respectively as the real and imaginary components of the ratio, $\sigma_0^B e^{i\delta} / \varepsilon_0^B$. We have determined these to be

$$E_{storage}(T,C,\omega) = \frac{\left(\beta_1(T,C)-\omega^2\beta_1(T,C)\right)\left(\alpha_1(T,C)-\omega^2\alpha_1(T,C)\right)+\omega^2\alpha_2(T,C)\beta_2(T,C)}{\left(\alpha_1(T,C)-\omega^2\alpha_1(T,C)\right)^2+\omega^2\alpha_2^2(T,C)} \quad ,$$
$$E_{loss}(T,C,\omega) = \frac{\omega\left[-\alpha_2(T,C)\left(\beta_1(T,C)-\omega^2\beta_1(T,C)\right)+\beta_2(T,C)\left(\alpha_1(T,C)-\omega^2\alpha_1(T,C)\right)\right]}{\left(\alpha_1(T,C)-\omega^2\alpha_1(T,C)\right)^2+\omega^2\alpha_2^2(T,C)} \quad . \tag{30}$$

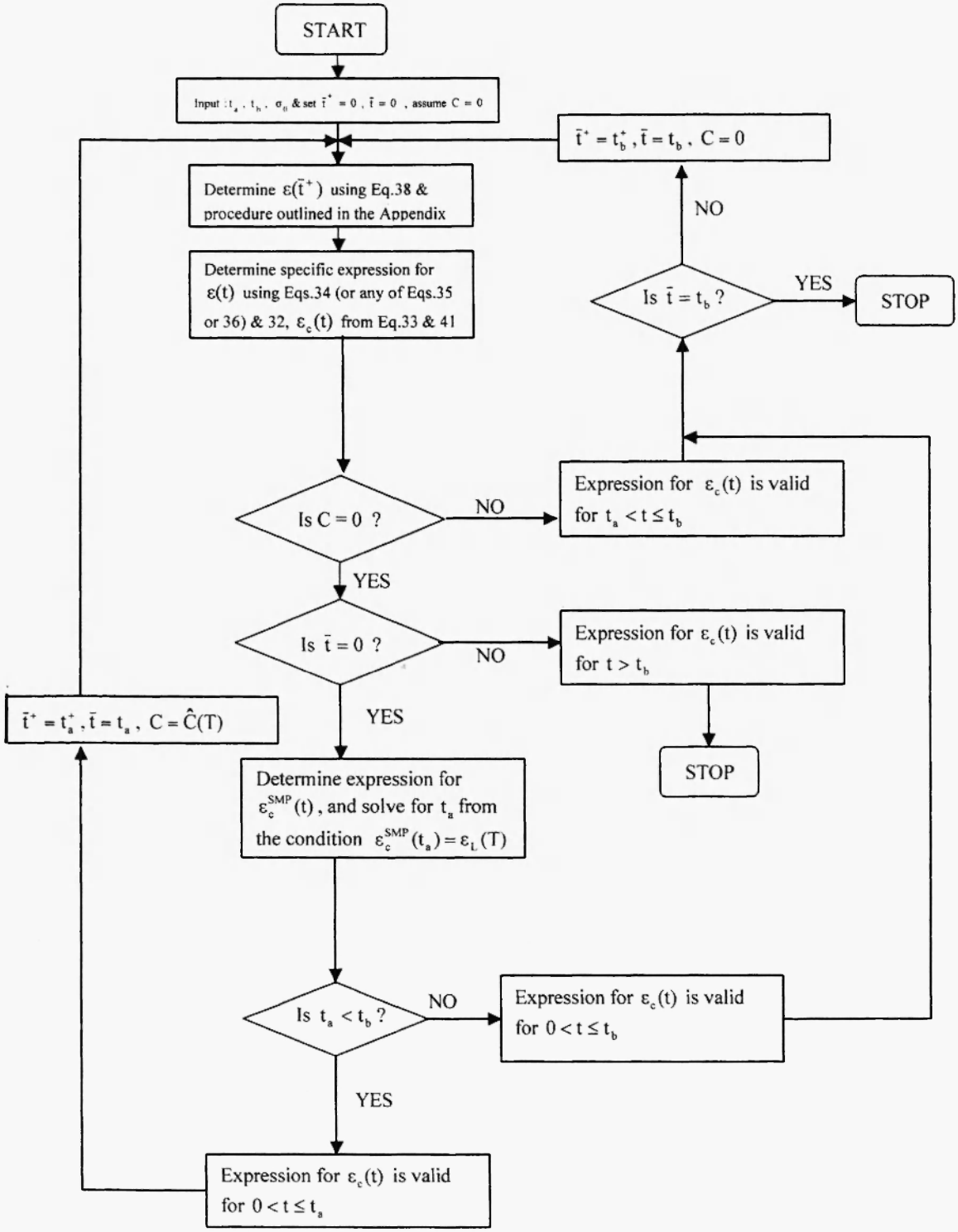

Fig. 5: The flowchart for the computational procedure.

The loss angle may be determined from the definition, $\delta = \tan^{-1}\frac{E_{loss}}{E_{storage}}$. Using Equation 30, it is

$$\delta(T,C,\omega) = \tan^{-1}\frac{\omega\left[-\alpha_2(T,C)\left(\beta_3(T,C)-\omega^2\beta_1(T,C)\right)+\beta_2(T,C)\left(\alpha_3(T,C)-\omega^2\alpha_1(T,C)\right)\right]}{\left(\beta_3(T,C)-\omega^2\beta_1(T,C)\right)\left(\alpha_3(T,C)-\omega^2\alpha_1(T,C)\right)+\omega^2\alpha_2(T,C)\beta_2(T,C)} \quad . \tag{31}$$

Note that if the friction element is active (the second of Equation 2), then $C = \hat{C}(T)$ whereas if it is inactive (the first and third of Equation 2), then C = 0. Therefore, during the periodic loading, the loss angle will follow from Equation 31 corresponding to either $C = \hat{C}(T)$ or C = 0. Specific expressions for the loss angles of some selected models will be given in Section 5.

5. OVERALL SHAPE MEMORY STRAIN AND DAMPING FOR THE SPRING-SMP HYBRID MODELS

In order to ascertain the interactions of the SMP with a purely elastic inactive material (the linear spring), we shall focus on the series and parallel combinations of the SMP with the spring. The explicit expressions are given for overall shape memory strain (generated using Equations 20-27) and damping capacity (in terms of the loss angle). For completeness, we shall also include the explicit expressions pertaining to the shape memory polymer.

5.1 The Shape Memory Polymer

The creep strain of the shape memory polymer is determined to be

$$\varepsilon_c^{SMP}(t) = \begin{cases} \sigma_0\left[\dfrac{1}{E_2(T)}-\dfrac{1}{E(T)}\right]\left(1-e^{-t/\lambda(T)}\right) & \text{for} \quad 0<t<t_a \quad \text{and} \quad t_a \le t_b \\ \varepsilon_L(T) + \sigma_0\left[\dfrac{\varepsilon_{s,eff}(T,\hat{C})-\varepsilon_L(T)}{\sigma_0}+\dfrac{1}{E_{2,eff}(T,\hat{C})}-\dfrac{1}{E(T)}\right]\left(1-e^{-(t-t_a)/\lambda_{eff}(T,\hat{C})}\right) & \text{for} \quad t_a<t<t_b \\ \varepsilon_s(t_b,T) + \sigma_0\left[\varepsilon_c(t_b)-\varepsilon_s(t_b,T)\right]\left(1-e^{-(t-t_b)/\lambda(T)}\right) & \text{for} \quad t>t_b \end{cases} , \tag{32}$$

where t_a (see the first of Equation 32) is the time during the loading process when the creep strain in the SMP attains the value, $\varepsilon_L(T)$, and can be solved from the identity

$$\varepsilon_c^{SMP}(t_a) = \varepsilon_L(T) \quad . \tag{33}$$

This identity will also be invoked to determine t_a for the models discussed in Sections 5.2 and 5.3 below. The damping capacity of the SMP can be determined from its loss angle

$$\tan\delta^{SMP}(T,C,\omega) = \frac{\omega}{\mu(T)} \cdot \frac{1-\dfrac{E_2(T)}{E(T)}}{\dfrac{\omega^2}{E(T)} + \dfrac{1}{\mu_{eff}(T,C)\lambda_{eff}(T,C)}} \cdot \tag{34}$$

Eqs. 32 and 34 were originally given by Bhattacharyya and Tobushi (2000), and correspond to their Eqs.8 and 25 respectively. The specific values, $\delta^{SMP}(T,0,\omega)$ and $\delta^{SMP}(T,\hat{C},\omega)$, will correspond to the situation when the friction element is inactive and active respectively. This is also true for the damping capacity of the models given in Sections 5.2 and 5.3 below.

5.2 The Spring-SMP series hybrid

The creep strain of the spring-SMP series hybrid model turns out to be

$$\varepsilon_c(t) = (1-V_\Lambda)\,\varepsilon_c^{SMP}(t)\,, \tag{35}$$

where $\varepsilon_c^{SMP}(t)$ follows from Equation 32. The residual shape memory strain of the spring- SMP series hybrid is lower than that of the SMP itself. On the other hand, the loss angle is

$$\frac{\tan\delta(T,C,\omega)}{\tan\delta^{SMP}(T,C,\omega)} = \left[1 + \frac{V_{I\Lambda}}{V_\Lambda} \cdot \frac{E_{2.eff}(T,C)}{E_p} \cdot \frac{\dfrac{1}{\mu_{eff}(T,C)\lambda_{eff}(T,C)} + \dfrac{\omega^2}{E_{2.eff}(T,C)}}{\dfrac{1}{\mu_{eff}(T,C)\lambda_{eff}(T,C)} + \dfrac{\omega^2}{E(T)}}\right]^{-1}, \tag{36}$$

and for $0 < V_\Lambda < 1$, it is easy to see that the damping due to the SMP is higher than that of the spring-SMP series hybrid, i.e. $\tan\delta^{SMP}(T,C,\omega) > \tan\delta(T,C,\omega) > 0$.

5.3 The Spring-SMP parallel hybrid

The creep strain of the spring-SMP parallel hybrid model is

$$\varepsilon_c(t) := \begin{cases} \sigma_0\left(\dfrac{1}{V_A E_2(T)+V_{IA}E_p}-\dfrac{1}{V_A E(T)+V_{IA}E_p}\right)\left(1-e^{-\frac{1}{\lambda(T)}\cdot\frac{V_A+V_{IA}\frac{E_p}{E_2(T)}}{V_A+V_{IA}\frac{E_p}{E(T)}}t}\right) & \text{for } 0<t<t_a \text{ and } t_a \le t_b \\ \varepsilon_c(t_a)+\sigma_0\left(\dfrac{V_A}{V_A+V_{IA}\frac{E_p}{E_{2,eff}(T,C)}}\dfrac{\varepsilon_{s,eff}(T,C)}{\sigma_0}-\dfrac{\varepsilon(t_a)}{\sigma_0}\right)\dfrac{1}{E_{2,eff}(T,C)}\left(V_A+V_{IA}\dfrac{E_p}{E_{2,eff}(T,C)}\right)^{-1}\times & \\ \left(1-e^{-\frac{1}{\lambda_{eff}(T,C)}\cdot\frac{V_A+V_{IA}\frac{E_p}{E_{2,eff}(T,C)}}{V_A+V_{IA}\frac{E_p}{E(T)}}(t-t_a)}\right) & \text{for } t_a<t<t_b \\ \varepsilon_c(t_b)+\sigma_0\left(\dfrac{V_A}{V_A+V_{IA}\frac{E_p}{E_2(T)}}\varepsilon_s(t_b,T)-\varepsilon_c(t_b)\right)\left(1-e^{-\frac{1}{\lambda(T)}\cdot\frac{V_A+V_{IA}\frac{E_p}{E_2(T)}}{V_A+V_{IA}\frac{E_p}{E(T)}}(t-t_b)}\right) & \text{for } t>t_b \end{cases} \tag{37}$$

The damping capacity is given by

$$\frac{\tan\delta(T,C,\omega)}{\tan\delta^{SMP}(T,C,\omega)}=\left[1+\frac{V_{IA}}{V_A}\frac{E_p}{E(T)}\right]^{-1}\left[1+\frac{V_{IA}E_p\left(\frac{1}{E_{2\,eff}(T,C)}-\frac{1}{E(T)}\right)}{V_A+V_{IA}\frac{E_p}{E(T)}}\right]^{-1}, \tag{38}$$

$$1+\omega^2\frac{\mu_{eff}(T,C)\lambda_{eff}(T,C)}{E(T)}$$

where it is clear that for $0 < V_{IA} < 1$, $\tan\delta^{SMP}(T,C,\omega) > \tan\delta(T,C,\omega) > 0$.

6. PARAMETRIC STUDIES OF THE SMP-BASED COMPOSITES

In Sections 6.1 and 6.2, we give parametric studies on the creep strain and damping capacity of the SMP-spring hybrid models. In fact, recall that since the SMP-spring series model and the SMP-spring parallel

model can represent a composite laminate and an aligned fiber composite respectively (both loaded uniaxially as shown in Figures 2a and b), the parametric studies shall focus on the effect of the volume fraction, V_{IA}, and the Young's modulus, E_p, of the inactive elastic phase on the overall composite response.

The specific material properties of the SMP that we shall use are those of a shape memory polyurethane of the polyester polypole series characterized by Tobushi *et al.* (1997). The material properties of the polymer show a significant temperature dependence in a narrow temperature range around its glass transition temperature, T_g. The lower and upper values of this range are taken as T_L and T_H respectively, i.e. $T_L < T_g < T_H$. The temperature dependence of the properties outside this range is not as significant and will be neglected (see Figure 4a, Tobushi *et al.*, 1997). For the purpose of modeling, it was found that within the range, an exponential temperature dependence of all material properties was a reasonable approximation. In particular, the specific form of E(T) is taken as

$$E(T) = \begin{cases} E_g e^{A_g\left(\frac{T_g}{T} - 1\right)} & E(T_L) \\ & \text{for } T_L < T < T_H \\ E(T_H) & \text{for } T > T_H \end{cases}, \tag{39}$$

where all temperature parameters are taken in Kelvin. The temperature dependence of the remaining parameters, i.e. $\mu(T), \lambda(T), C(T), \varepsilon_L(T)$ follow from Equation 39 by replacing the letter "E" with μ, λ, C and ε_L respectively. This replacement is also done for the subscript "E" of A_E in the second of Equation 39. The specific numerical values of the parameters of the shape memory polyurethane tested by Tobushi *et al.* (1997) are given in Table 1, and are used for the parametric studies in the sequel.

6.1 Creep strain ratio of SMP- based Composites

In this section, we study the effect of the inactive elastic phase on the creep response of the SMP-based composite. For brevity, we focus on the residual creep strain in the composite at $t \to \infty$. For the SMP itself, Equation 32 may be used to show that $\varepsilon_c^{SMP}(\infty) = \varepsilon_s(t_b, T)$. With this result, Equation 35 reduces to

$$\frac{\varepsilon_c(\infty)}{\varepsilon_c^{SMP}(\infty)} = 1 - V_{IA}, \tag{40}$$

for the composite laminate whereas Equation 37 reduces to

$$\frac{\varepsilon_c(\infty)}{\varepsilon_c^{SMP}(\infty)} = \left[1 + \frac{V_{IA}}{V_A}\frac{E_p}{E_s(T)}\right]^{-1}, \tag{41}$$

for the aligned fiber composite. The ratio, $\varepsilon_c(\infty)/\varepsilon_c^{SMP}(\infty)$, as a function of $V_{I\Lambda}$ and E_p is the residual creep strain of the composite relative to the SMP; we shall refer to it as the creep strain ratio. In either case, it is clear that as long as there is an inactive elastic phase ($V_{I\Lambda} \neq 0$), the creep strain ratio is less than 1.

Equation 40 clearly states that the creep strain ratio for the composite laminate is linearly dependent on the volume fraction of the inactive elastic phase, and is independent of its stiffness, E_p. In Figure 6, we have plotted the creep strain ratio for the aligned fiber composite (Eq.41) at $T = T_g$ with respect to $V_{I\Lambda}$ at different values of $E_p/E(T_g)$. With the focus on examining the effect of a stiffer inactive elastic phase, we have restricted E_p to $E_p/E(T_g)>1$. We shall adhere to this restriction in the entire parametric study. It is quite apparent that even a moderately stiffer inactive elastic phase (e.g. $E_p/E(T_g) = 10$) results in a significant drop in the creep strain, and that too when the volume fraction of the inactive phase is quite small (less than 10%). The plot of the creep strain ratio with respect to $E_p/E(T_g)$ at various volume fractions of the inactive phase has been given in Figure 7 and it is seen that the creep ratio tends to approach a certain asymptotic value beyond which an increase in the inactive phase stiffness does not produce a noticeable change in the composite creep strain ratio.

6.2 Damping capacity ratio of SMP-based Composites

In this section, we present the results of the analysis of the damping capacity ratio, $\tan\delta(T,C,\omega)/\tan\delta^{SMP}(T,C,\omega)$ for the composite laminate (see Equation 36) in Figures 8 and 9. The damping capacity ratio has been plotted in Figure 8 with respect to $V_{I\Lambda}$ at three different temperatures, T = 323 K , 328 K and 333 K (Recall that T_g= 328 K). In all these cases, the stiffness of the inactive phase has been set such that $E_p/E(T_g) = 10$, the frequency is fixed at $\omega = 1$ Hz and $C = 0$ (no evolving irrecoverable

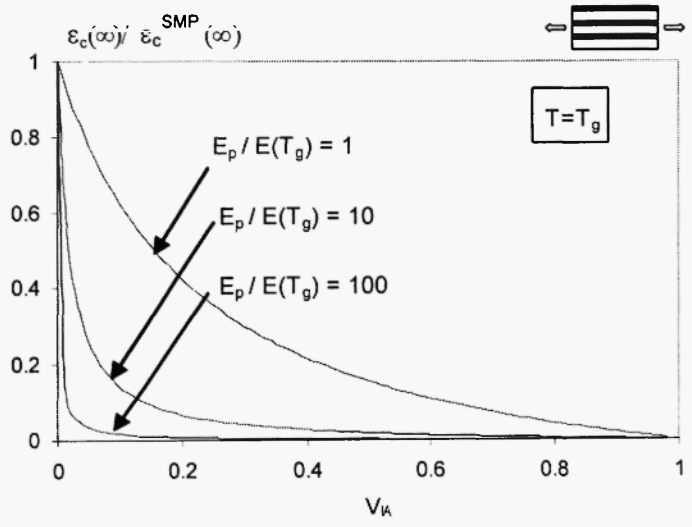

Fig. 6: The creep strain ratio as a function of the volume fraction of the inactive elastic phase, for the aligned fiber composite.

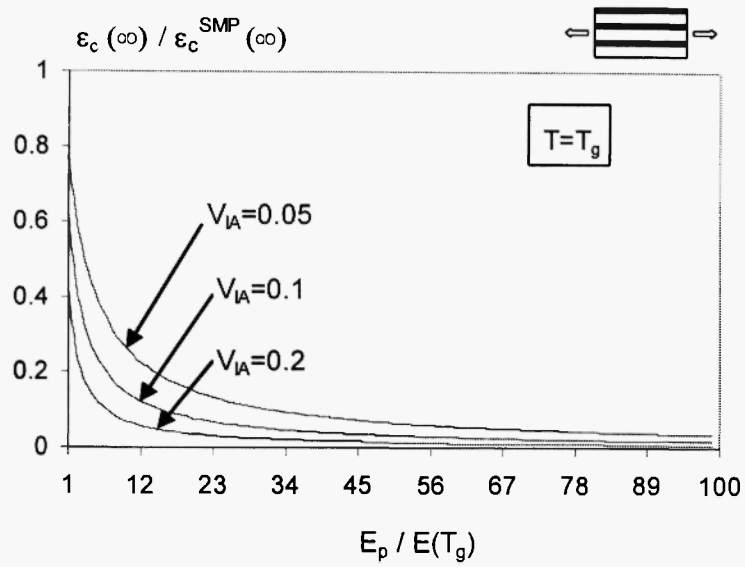

Fig. 7: The damping capacity ratio as a function of the relative stiffness of the inactive elastic phase, for the aligned fiber composite.

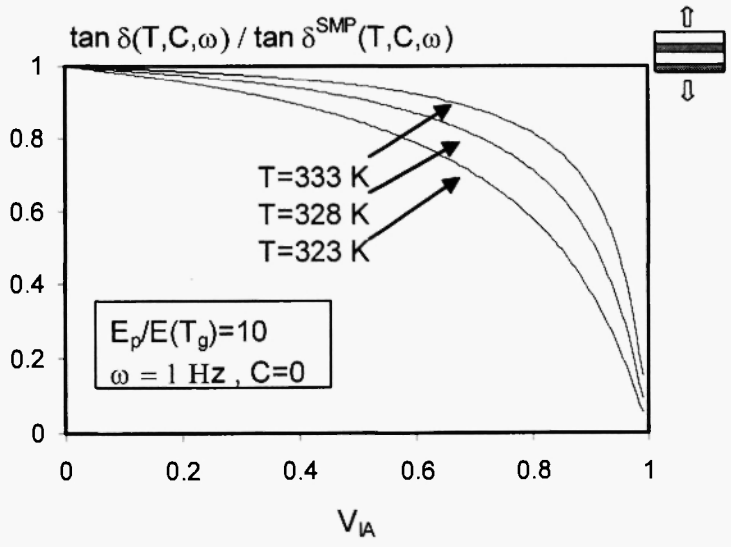

Fig. 8: The damping capacity ratio as a function of the volume fraction of the inactive elastic phase, for the composite laminate.

creep strain). While in all these cases, the presence of the inactive phase results in a reduction of the damping capacity ratio, an increase in the temperature increases the ratio. Another notable feature is that the reduction is relatively modest for a wide range of the volume fraction, up to about $V_{IA} \sim 0.6$. The damping ratio has been plotted in Figure 9 with respect to the stiffness of the inactive phase at the three aforementioned

temperatures. In all these cases, the frequency has been set at 1 Hz and the volume fraction of the inactive phase at 50%, and C = 0 (no evolving irrecoverable creep strain). Notice that as the inactive elastic phase becomes less stiff, the damping capacity ratio decreases. In the limit, when the inactive phase is a void (with E_p = 0; not shown in the figure), Equation 36 states that the damping capacity ratio vanishes (and therefore the *damping capacity* of the SMP-based voided laminate vanishes). This is because for a given strain input, Equation 28, the resultant stress that the voided phase is able to sustain vanishes. Therefore, due to the laminate arrangement, the overall stress, Equation 29, vanishes too, i.e. $\sigma_0^B \to 0$. Thus, the dissipation also vanishes. Beyond this limiting case, as E_p is increased, there is an increase in the damping capacity ratio also. Note that the composite laminate quickly attains a substantial portion of the SMP damping capacity as $E_p/E(T_g)$ increases from 1 to 12. Further, an increase in temperature at any given value of $E_p/E(T_g)$ increases the damping capacity ratio of the composite. Note that the results in Figures 8 and 9 have been plotted at C = 0. We have numerically checked and found that the creep strain ratio and the damping capacity ratio do not visibly change even when there is an evolving creep strain (i.e. $C = \hat{C}(T)$). We have also repeated the calculations at a low frequency, w = 0.012 Hz and have found the ratios to have marginally higher values for all the different cases reported in Figures 8 and 9.

The damping capacity ratio for the aligned fiber composite (see Equation 38) has been plotted in Figure 10 with respect to V_{IA}. Three plots corresponding to three different temperatures – 323 K, 328 K and 333 K – have been given, all at $E_p/E(T_g)$=10, ω = 1 Hz and C = 0. In contrast to the composite laminate (Figure 8), it is seen that the damping capacity ratio decreases with a higher temperature. Another feature of contrast is that beyond a certain amount of the inactive phase, e.g. V_{IA}~ 0.05, there is a substantial reduction of the damping capacity of the composite. Finally, the evolution of the damping capacity ratio as a function of $E_p/E(T_g)$ has been given in Fig. 11 at the three different aforementioned temperatures. All the three plots are at V_{IA} = 0.5, ω = 1 Hz and C = 0. In contrast to the composite laminate (Figure 9), the damping capacity ratio for the aligned fiber composite approaches 1 in the limiting case of a void, $E_p \to 0$. This is because even if the inactive elastic phase in the aligned fiber composite cannot sustain any stress in the limiting case of vanishing stiffness, the geometrical arrangement of the two phases does not in any way hinder the capacity for the SMP to sustain an oscillatory stress in response to an oscillatory strain imposed on the entire composite. The composite, in that case, has a damping capacity identical to that of the SMP itself. As $E_p/E(T_g)$ increases, there is a reduction in the damping capacity ratio, and a significant reduction occurs fairly quickly, as $E_p/E(T_g)$, for example, attains a value of 12.

6.3 Design Strategies of SMP-based Composites

The stiffness of shape memory polymers is usually low. Thus, for example, the Young's modulus, ET_g), of the SMP at its glass transition temperature follows from Eq. 39 and Table 1 as 146 MPa. The low stiffness may be compensated if the SMP is combined with a stiffer material (e.g. an inactive elastic phase). An immediate consequence will be that the creep strain and the damping capacity of the composite will be lower

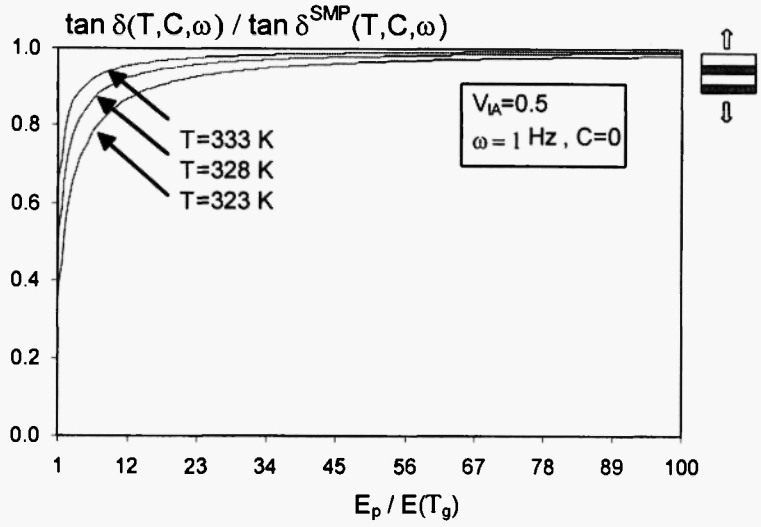

Fig. 9: The damping capacity ratio as a function *of* the relative stiffness of the inactive elastic phase, for the composite laminate.

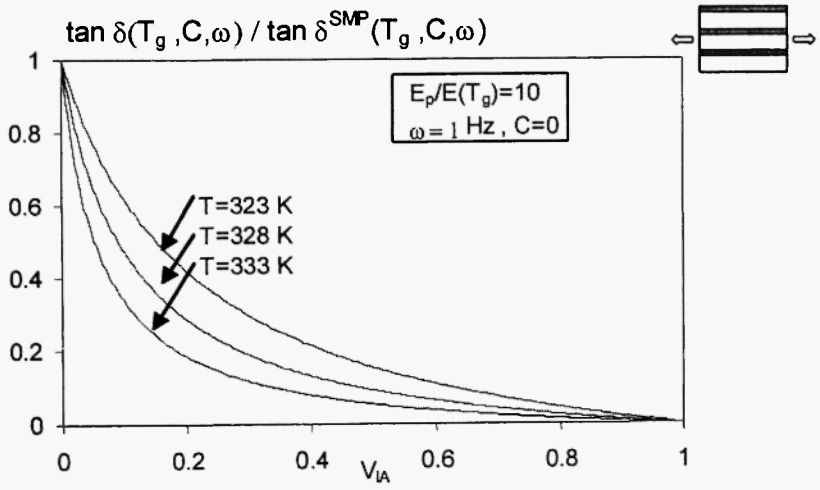

Fig. 10: The damping capacity ratio as a function of the volume fraction of the inactive elastic phase, for the aligned fiber composite.

than the corresponding values for the SMP; the question is to what extent? We shall partially address this question now.

The overall elastic modulus, $E^{comp}(T)$, of the composite laminate and the aligned fiber composite is identified from Eq.26 as $\beta_2(T,C)/\alpha_2(T,C)$. Then, using Eqs. 14 and 16, we have

$$\frac{E^{comp}(T)}{E(T)} = \begin{cases} \left[V_A + V_{IA} \dfrac{E(T)}{E_p} \right]^{-1} & \text{for composite laminate} \\ V_A + V_{IA} \dfrac{E_p}{E(T)} & \text{for aligned fiber composite} \end{cases} \tag{42}$$

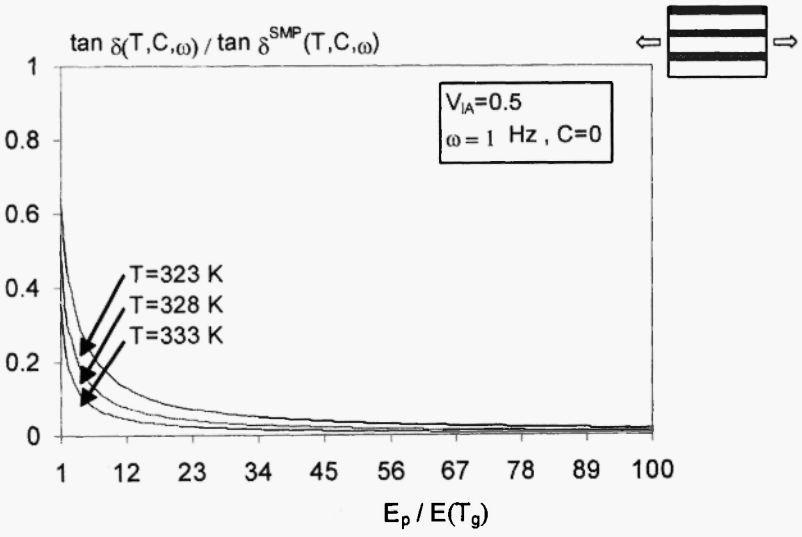

Fig. 11: The damping capacity ratio as a function of the relative stiffness of the inactive elastic phase, for the aligned fiber composite.

Consider a composite laminate with $V_{IA} = 0.5$ and $E_p/E(T_g) = 2.64$ and an aligned fiber composite with $V_{IA} = 0.05$ and $E_p/E(T_g) = 10$. The composite stiffness for either geometrical arrangement is identical (check using Eq.42), i.e. $E^{comp}(T)/E(T) = 1.45$. However, at $T = T_g$, the composite laminate has higher ratios of creep strain and damping capacity (50% and 72.53 %) than the aligned fiber composite (26% and 65.52 %). In general, a composite laminate seems to offer a better retention of the SMP creep strain and damping capacity over a wide range of the inactive phase volume fraction and stiffness, and should therefore be preferred over the aligned fiber arrangement. A more definitive answer can emerge once an optimization problem involving the composite stiffness, creep strain and the damping capacity is addressed. That is beyond the scope of this paper.

Table 1

A list of material properties of a shape memory polyurethane of the polyester polypole series (Tobushi *et al.*,1997).

Symbol	Value
T_g	328 K
$T_{l,}$	313 K
T_{ll}	343 K
E_g	146 MPa
μ_g	14 GPa.s
λ_g	521 s
C_g	0.112
$\varepsilon_{l,g}$	0.3%
$A_{t;}$	38.1
A_μ	44.2
A_λ	35.4
A_c	38.7
$A_{\varepsilon_{l,}}$	-58.2

CONCLUSIONS

This paper has provided a generalized methodology for the analytical determination of the isothermal uniaxial mechanical response of a shape memory polymer (SMP) in series and parallel arrangements with a spring, dashpot, a Maxwell solid and a Kelvin solid. We have shown analytically that four models - the SMP-spring series hybrid, the SMP-spring parallel hybrid, the SMP-Kelvin solid series hybrid and the SMP-Maxwell solid parallel hybrid - demonstrate an effective response similar to that of a SMP itself. Explicit expressions for the creep strain and the damping capacity are provided for the SMP-spring and SMP-dashpot hybrids. Parametric studies of the SMP-spring series and parallel hybrids yield information about the effective response of SMP-based composite laminates and aligned fiber composites respectively.

ACKNOWLEDGEMENTS

This work has been supported by the National Sciences and Engineering Research Council of Canada through their operating grant to A.B.

A1. APPENDIX:

Model parameters for the dashpot-SMP, Maxwell solid-SMP and Kelvin solid-SMP models.

A1.1 *The dashpot-SMP series hybrid*

$$\alpha_1(T,C)=\frac{V_{\dot{}}}{E(T)}\quad,\quad \alpha_2(T,C)=\frac{V_{IA}}{\eta_p}+\frac{V_A}{\mu_{eff}(T,C)}\quad,\quad \alpha_3(T,C)=\frac{V_{IA}}{\eta_p\mu_{eff}(T,C)}\quad,$$
$$\beta_1(T,C)=1\quad,\quad \beta_2(T,C)=\frac{1}{\lambda_{eff}(T,C)}\quad,\quad \beta_3(T,C)=0\quad, \tag{43}$$
$$\varepsilon_s^{total}(T,C)=0\quad,$$

$$\varepsilon_c^{SMP}(t)=\begin{cases}0 & \text{when} \quad V_A=0\\ \dfrac{1}{V_A}\left[\varepsilon(t)-\dfrac{V_{IA}}{\eta_p}\int_0^t\sigma(\tilde{t})\,d\tilde{t}\right]-\dfrac{\sigma(t)}{E(T)} & \text{when} \quad V_A\neq 0\end{cases}. \tag{44}$$

A1.2 *The Maxwell solid-SMP series hybrid*

$$\alpha_1(T,C)=\frac{V_{\dot{}}}{E(T)}+\frac{V_{\dot{}\dot{}}}{E_{\dot{}}}\quad,\quad \alpha_2(T,C)=\frac{V_A}{\mu_{eff}(T,C)}+V_{IA}\left(\frac{1}{\eta_p}+\frac{1}{E_p\lambda_{eff}(T,C)}\right)\quad,$$
$$\alpha_3(T,C)=\frac{V_{IA}}{\eta_p\mu_{eff}(T,C)}\quad, \tag{45}$$
$$\beta_1(T,C)=1\quad,\quad \beta_2(T,C)=\frac{1}{\lambda_{eff}(T,C)}\quad,\quad \beta_3(T,C)=0\quad,$$
$$\varepsilon_s^{total}(T,C)=0\quad,$$

$$\varepsilon_c^{SMP}(t)=\begin{cases}0 & \text{when} \quad V_A=0\\ \dfrac{1}{V_A}\left[\varepsilon(t)-\dfrac{V_{IA}}{\eta_p}\int_0^t\sigma(\tilde{t})\,d\tilde{t}-\dfrac{V_{IA}}{E_p}\sigma(t)\right]-\dfrac{\sigma(t)}{E(T)} & \text{when} \quad V_A\neq 0\end{cases}. \tag{46}$$

A1.3 *The Kelvin solid-SMP series hybrid*

$$\alpha_1(T,C)=0 \quad , \quad \alpha_2(T,C)=\frac{1}{a_5(T,C)}\left[\frac{1}{E(T)}+\frac{1}{V_A\lambda_{eff}(T,C)}\left(V_A\lambda_{eff}(T,C)-\frac{V_{IA}\eta_p}{E(T)}\right)a_1(T,C)\right] ,$$

$$\alpha_3(T,C)=\frac{1}{V_A\, a_5(T,C)\,\lambda_{eff}(T,C)}\left[\left(V_A\lambda_{eff}(T,C)-\frac{V_{IA}\eta_p}{E(T)}\right)a_2(T,C)+\frac{V_A}{E_p}+\frac{V_{IA}}{E_{2\,eff}(T,C)}\right] ,$$

$$\beta_1(T,C)=0 \quad , \quad \beta_2(T,C)=1 \quad , \quad \beta_3(T,C)=\frac{1}{V_A\, a_5(T,C)\,\lambda_{eff}(T,C)}\left[1-\left(V_A\lambda_{eff}(T,C)-\frac{V_{IA}\eta_p}{E(T)}\right)a_4(T,C)\right] ,$$

$$\varepsilon_s^{total}(T,C)=V_A\cdot\frac{1-\left(\lambda_{eff}(T,C)-\dfrac{V_{IA}\eta_p}{V_A E(T)}\right)a_5(T,C)}{1-\left(V_A\lambda_{eff}(T,C)-\dfrac{V_{IA}\eta_p}{E(T)}\right)a_4(T,C)}\;\varepsilon_{s,eff}(T,C) , \tag{47}$$

$$\varepsilon_c^{SMP}(t):=\begin{cases}0 & \text{when} \quad V_A=0\\ \left[\dfrac{\eta_p}{E_p}\dfrac{V_{IA}}{V_A}a_2(T,C)-\dfrac{V_{IA}}{V_A E_p}-\dfrac{1}{E(T)}\right]\sigma(t)\\ +\dfrac{1}{V_A}\left(1+V_A\dfrac{\eta_p}{E_p}a_4(T,C)\right)\left[\varepsilon(t)-V_A\left(1+V_{IA}\dfrac{E_p}{\eta_p}a_4(T,C)\right)^{-1}a_5(T,C)\varepsilon_{s,eff}(T,C)\right]\\ +\dfrac{\eta_p}{E_p}\dfrac{V_{IA}}{V_A}\left[a_3(T,C)\,\dot{\varepsilon}(t)+a_2(T,C)\,\dot{\sigma}(t)\right], \quad \text{when} \quad V_A\neq 0\end{cases} \tag{48}$$

where the parameters $a_1(T,C)$, $a_2(T,C)$, $a_3(T,C)$, $a_4(T,C)$ and $a_5(T,C)$ are

$$a_1(T,C)=-\frac{V_A\, a_3(T,C)}{E(T)} \;,\; a_2(T,C)=-\frac{a_3(T,C)}{E(T)\,\mu_{eff}(T,C)}\left(E_{2\,eff}(T,C)+V_A E_p\right) ,$$

$$a_3(T,C)=\mu_{eff}(T,C)\left[V_A\,\eta_p+V_{IA}\,\mu_{eff}(T,C)-\frac{\eta_p}{E(T)}\left(V_{IA}E_{2\,eff}(T,C)+V_A E_p\right)\right]^{-1} , \tag{49}$$

$$a_4(T,C)=\frac{1}{\lambda_{eff}(T,C)}a_3(T,C) \;,\; a_5(T,C)=V_A a_4(T,C) \;.$$

A1.4 *The dashpot-SMP parallel hybrid*

$$\alpha_1(T,C)=0\ ,\quad \alpha_2(T,C)=\frac{1}{E(T)}\ ,\quad \alpha_3(T,C)=\frac{1}{\mu_{eff}(T,C)}\ ,$$
$$\beta_1(T,C)=V_{IA}\frac{\eta_p}{E(T)}\ ,\ \beta_2(T,C)=V_A+V_{IA}\frac{\eta_p}{\mu_{eff}(T,C)}\ ,\ \beta_3(T,C)=\frac{V_A}{\lambda_{eff}(T,C)}\ , \tag{50}$$
$$\varepsilon_s^{total}(T,C)=\varepsilon_{s,eff}(T,C),$$

$$\varepsilon_c^{SMP}(t)=\begin{cases}0 & \text{when} \quad V_A=0\\ \varepsilon(t)+\dfrac{V_{IA}}{V_A}\dfrac{\eta_p}{E(T)}-\dfrac{\sigma(t)}{V_A E(T)}\dot{\varepsilon}(t) & \text{when} \quad V_A\neq 0\end{cases}. \tag{51}$$

A1.5 *The Maxwell solid-SMP parallel hybrid*

$$\alpha_1(T,C)=0\ ,\quad \alpha_2(T,C)=\frac{V_A\mu_{eff}(T,C)}{\varphi(T,C)E(T)}+\frac{\psi(T,C)}{\varphi(T,C)E(T)}\left(\frac{\mu_{eff}(T,C)}{E(T)}-\frac{\eta_p}{E_p}\right)\left(1+\frac{V_{IA}\eta_p}{V_A\mu_{eff}(T,C)}\right)^{-1},$$
$$\alpha_3(T,C)=1+\frac{\psi(T,C)}{V_A\varphi(T,C)\mu_{eff}(T,C)}\left(\frac{V_A\mu_{eff}(T,C)}{E(T)}-\frac{V_{IA}\eta_p}{E_p}\right)\left(1+\frac{V_{IA}\eta_p}{V_A\mu_{eff}(T,C)}\right)^{-1},$$
$$\beta_1(T,C)=0\ ,\ \beta_2(T,C)=1\ , \tag{52}$$
$$\beta_3(T,C)=\frac{V_A E_{2,eff}(T,C)}{\varphi(T,C)}+\frac{\psi(T,C)}{\varphi(T,C)\lambda_{eff}(T,C)}\left(\frac{V_A\mu_{eff}(T,C)}{E(T)}-\frac{V_{IA}\eta_p}{E_p}\right)\left(1+\frac{V_{IA}\eta_p}{V_A\mu_{eff}(T,C)}\right)^{-1},$$
$$\varepsilon_s^{total}(T,C)=\varepsilon_{s,eff}(T,C),$$

$$\varepsilon_c^{SMP}(t)=\begin{cases}0 & \text{when} \quad V_A=0\\ \varepsilon(t)-\dfrac{1}{V_A E(T)}\sigma(t)+\dfrac{V_{IA}\eta_p}{V_A E(T)}\dot{\varepsilon}(t)-\dfrac{V_{IA}\eta_p\psi(T,C)}{V_A E(T)E_p}\times & \\ \left\{\dot{\varepsilon}(t)-\left(1+\dfrac{V_{IA}\eta_p}{V_A\mu_{eff}(T,C)}\right)^{-1}\left[\left(\dfrac{\sigma(t)}{\mu_{eff}(T,C)}+\dfrac{\dot{\sigma}(t)}{E(T)}\right)\dfrac{1}{V_A}-\dfrac{1}{\lambda_{eff}(T,C)}\left(\varepsilon(t)-\varepsilon_{s,eff}(T,C)\right)\right]\right\} & \\ & \text{when} \quad V_A\neq 0\end{cases},$$

$$\psi(T,C)=\left[\frac{1}{E_p}-\frac{\dfrac{V_A}{E_p}+\dfrac{V_{IA}}{E(T)}}{V_A+\dfrac{V_{IA}\eta_p}{\mu_{eff}(T,C)}}\right]^{-1}\quad\text{and} \tag{53}$$

$$\varphi(T,C)=V_{IA}\eta_p+V_A\mu_{eff}(T,C)+\psi(T,C)\left(\frac{V_A\mu_{eff}(T,C)}{E(T)}-\frac{V_{IA}\eta_p}{E_p}\right).$$

A1.6 The Kelvin solid-SMP parallel hybrid

$$\alpha_1(T,C)=0 \quad , \quad \alpha_2(T,C)=\frac{1}{E(T)} \quad , \quad \alpha_3(T,C)=\frac{1}{\mu_{eff}(T,C)} \quad ,$$

$$\beta_1(T,C)=\frac{V_{IA}\eta_p}{E(T)} \quad , \quad \beta_2(T,C)= V_A + V_{IA}\left(\frac{\eta_p}{\mu_{eff}(T,C)}+\frac{E_p}{E(T)}\right), \tag{54}$$

$$\beta_3(T,C)=\frac{V_A}{\lambda_{eff}(T,C)}+\frac{V_{IA}E_p}{\mu_{eff}(T,C)},$$

$$\tilde{\varepsilon}_s^{total}(T,C)=\frac{V_A\, E_{2,eff}(T,C)}{V_A E_p + V_{IA}\, E_{2,eff}(T,C)}\varepsilon_{s,eff}(T,C),$$

$$\varepsilon_c^{SMP}(t) := \begin{cases} 0 & \text{when} \quad V_A = 0 \\ \left[1+\dfrac{V_{IA}E_p}{V_A E(T)}\right]\varepsilon(t)+\dfrac{V_{IA}\eta_p}{V_A E(T)}\dot{\varepsilon}(t)-\dfrac{1}{V_A E(T)}\sigma(t) & \text{when} \quad V_A \neq 0 \end{cases} . \tag{55}$$

A2. APPENDIX:

Determination of $\Delta\varepsilon(t)$ and $\Delta\dot{\varepsilon}(\bar{t})$ for the dashpot-SMP series hybrid model.

The jumps, $\Delta\varepsilon(t)$ and $\Delta\dot{\varepsilon}(\bar{t})$ (see comment in the last paragraph of Sec.4.1) will now be determined for the dashpot-SMP series hybrid model. A schematic of the model has been shown in Fig.4; also included are variables (or parameters) that represent the stresses and strains in the constituent elements. Note that the increments in stresses and strains over any time increment will be related through the usual constitutive relations for each component in the model. For the vanishingly small time interval under consideration, we have the following results

$$\Delta\varepsilon_2(\bar{t})=0 \quad , \quad \Delta\varepsilon_3(\bar{t})=0 \quad , \quad \Delta\dot{\sigma}(t)=0 \quad , \quad \Delta\varepsilon_s(\bar{t},T)=0, \tag{56}$$

where the first identity follows from $\Delta\varepsilon_2(\bar{t})=\lim_{\Delta\bar{t}\to 0}\int_{\bar{t}}^{\bar{t}+\Delta\bar{t}}\dot{\sigma}(\tilde{t})d\tilde{t}$, which vanishes as long as $\sigma(t)$ is finite during the time interval under consideration. The jump, $\Delta\varepsilon_3(\bar{t})$, also vanishes for the same reason. For the piecewise-constant stress input, the jump in the stress rate, $\Delta\dot{\sigma}(t)$, is zero. Finally, the last condition follows from the fact that the irrecoverable creep strain cannot change during a vanishingly small time interval (as long as stress and strain rates are finite). With the identities in Eq.56, and the constitutive relations of the model components, the following relations can be written

$$
\begin{aligned}
&\Delta\varepsilon(\bar{t}) = V_A\,\Delta\varepsilon_1(\bar{t}) = V_A\Delta\varepsilon_4(\bar{t})\ ,\\
&\Delta\sigma(\bar{t}) = \Delta\sigma_1(\bar{t}) + \Delta\sigma_2(\bar{t})\ ,\\
&\Delta\sigma_1(\bar{t}) = \eta(T)\Delta\dot{\varepsilon}_3(\bar{t})\ ,\\
&\Delta\sigma_1(\bar{t}) = E_1(T)\,\Delta\varepsilon_4(\bar{t})\ ,\\
&\Delta\dot{\varepsilon}_2(\bar{t}) = \Delta\sigma(\bar{t})/\eta_p\ ,\\
&\Delta\sigma_2(\bar{t}) = E_2(T)\,\Delta\varepsilon_1(\bar{t})\ ,\\
&\Delta\dot{\varepsilon}(\bar{t}) = V_A\,\Delta\dot{\varepsilon}_1(\bar{t}) + V_{IA}\Delta\dot{\varepsilon}_2(\bar{t})\\
&\qquad = V_A\,\Delta\dot{\varepsilon}_3(\bar{t}) + V_A\,\Delta\dot{\varepsilon}_4(\bar{t}) + V_{IA}\Delta\dot{\varepsilon}_2(\bar{t})\ ,\\
&0 = \Delta\dot{\sigma}_1(\bar{t}) + \Delta\sigma_2(\bar{t})\ .
\end{aligned}
\tag{57}
$$

Note from the first, second, fourth and sixth of Eq.57 that

$$
\Delta\varepsilon(\bar{t}) = V_A\,\frac{\Delta\sigma(\bar{t})}{E_1(T)+E_2(T)} = V_A\,\frac{\Delta\sigma(\bar{t})}{E(T)}\ , \tag{58}
$$

where the first of Eq. 7 has been used. The third, fourth, fifth and eighth in the seventh of Eq. 57 lead to

$$
\Delta\dot{\varepsilon}(\bar{t}) = V_A\,\frac{\Delta\sigma_1(t)}{\eta(T)} - V_A\,\frac{\Delta\dot{\sigma}_2(t)}{E_1(T)} + V_{IA}\,\frac{\Delta\sigma(\bar{t})}{\eta_p}\ . \tag{59}
$$

The first and fourth of Eq.57 along with Eq. 58 give $\Delta\sigma_1(t) = \dfrac{E_1(T)}{E(T)}\Delta\sigma(t)$. Using this result, Eq. 59 can be rewritten as below once we use the fifth, sixth and seventh of Eq. 57

$$
\Delta\dot{\varepsilon}(\bar{t}) = \left[\frac{V_{IA}}{\eta_p} + \frac{V_A}{\eta(T)}\left(\frac{E_1(T)}{E(T)}\right)^2\right]\Delta\sigma(t)\ , \tag{60}
$$

where the first of Eq. 7 has been used. Eqs. 58 and 60 are the desired jumps in the total strain and total strain rates respectively in terms of the material parameters of the model and the total stress input.

REFERENCES

1. A. Bhattacharyya and H. Tobushi, *Polymer Engineering and Science,* **40** (12), 2498 (2000).
2. W.N. Findley, J.S. Lai and K. Onaran, *Creep and Relaxation Behavior of Nonlinear Viscoelastic Materials,* Dover, 1976.

3. R.F. Gordon, *Proceedings of the 1st International Conference on Shape Memory and Superelastic Technologies*, Pacific Grove, California, A.R. Pelton, D. Hodgson and T. Duerig (Eds), 1994; p.15.
4. S. Hayashi, S. Kondo, P. Kapadia and E. Ushioda, *Plastics Engineering,* 29 (1995).
5. C. Liang, C.A. Rogers and E. Malafeew, *Smart Struct. Mater.* AD-24/ AMD-123, 97 (1991).
6. H.Tobushi, H. Hara, E. Yamada and S. Hayashi, *Smart Mater. Struct.,* **5,** 483 (1996).
7. H. Tobushi, T. Hashimoto, S. Hayashi and E. Yamada, E., *J. Intell. Mater. Sys. Struct.,* **8**, 711(1997).
8. H. Tobushi, S. Hayashi and P.H. Lin, *Proceedings of the 1st International Conference on Shape Memory and Superelastic Technologies*, Pacific Grove, California, A.R. Pelton, D. Hodgson and T. Duerig (Eds), 1994; p.109.
9. H. Tobushi, K.Okumura, S.Hayashi and N. Ito, *Mechanics of Materials*, **33,** 545 (2001).